Proposition of correlations for the dynamic parameters of carbonate sands

Felipe Oscar Pinto Barroso[1#] (iD), Alfran Sampaio Moura[1] (iD)

Article

Keywords
Carbonate sands
Soil dynamic parameters
Shear strain modulus
Damping ratio
Multiple linear regression

Abstract
The offshore industry has been challenged with the necessity to build structures with foundations on carbonate soils, found in extensive areas of the tropical and intertropical zones of the planet. As a better understanding of the behavior of these soils becomes more and more indispensable, this paper presents equations to predict the dynamic behavior of carbonate sands, in which two expressions (G/G_{max} versus γ and D versus γ) were obtained via multiple linear regression using data from resonant column tests carried out on carbonate sands from Cabo Rojo, Puerto Rico (Cataño & Pando, 2010). The proposed equations agreed well with experimental data. The error for the expressions G/G_{max} versus γ was less than 10%, while the expressions D versus γ trended to underestimate the values for the loose condition ($D_r = 24\%$), presenting an effective confining stress of 50kPa. Furthermore, the proposed equations were compared with predictions exhibited by Javdanian & Jafarian (2018) of G/G_{max} versus γ and D versus γ for carbonate sands, also yielding fairly concordant results.

1. Introduction

Carbonate soils are found in extensive areas of the tropical and intertropical zones of the Earth, forming deep layers of limestone sediments (Hyodo et al., 1996). The offshore oil and gas industry has often faced the need to build and install structures with foundations laid on this type of soil, creating the demand to develop research in order to better understand the behavior of carbonate soils, as well as its divergences in relation to soils originated from quartz (King & Lodge, 1988 *apud* Sharma & Ismail, 2006).

Carbonate sands have a more ductile and contractive behavior. When compared to quartz sands and tested under similar conditions, they tend to reduce their volume during shearing. A better way to understand their behavior is through laboratory and field tests.

This study aimed at developing correlations to predict the dynamic parameters of carbonate sands – maximum shear modulus (G_{max}) and damping ratio (D) – using multiple linear regression, comparing the predictions obtained through the proposed equations for G/G_{max} versus γ (shear strain) and D versus γ with experimental data from other studies.

2. Soil dynamic parameters

Soil dynamic parameters are highly dependent on the imposed level of strain. The shear modulus (G), for example, can be 10 times smaller when going from a shear strain of 0.001% to 1% (Barros & Hachich, 1998). The ranges of shear strain values vary according to the engineering problems, varying between $10^{-4}\%$ (foundation of precise equipment) and $10^{-1}\%$ (offshore problems).

Soil dynamic parameters can be determined through laboratory and field tests. However, in order to get the proper values, it is necessary to consider the strain levels involved in the situation and then conduct the tests in the same strain magnitude. According to Barros & Hachich (1998), examples of laboratory tests that can be used to obtain the soil dynamic parameters are: resonant column, bender elements, cyclic simple shear, cyclic triaxial and cyclic torsion.

Usual field tests to obtain dynamic properties are based on seismic methods. They cause shear strains of less than 0.001% and provide parameters related to reduced strains, such as the maximum shear modulus. According to Barros & Hachich (1998), examples of field tests commonly used to determine soil dynamic properties are: crosshole, downhole, uphole, seismic piezocone and pressiometric test.

Ponte & Moura (2017) assessed methods that considered small and large strains to obtain soil dynamic parameters. The cited authors concluded that the G_{max} obtained through large strain methods (such as the Standard Penetration Test, *SPT*) was on average three times smaller than that estimated by small strain ones (such as the downhole test). Since G_{max} is associated with small shear strains, the study showed how crucial it is to use the appropriate scale when estimating soil parameters. Analyzing how G varies with shear strain, it is

possible to qualitatively evaluate the decrease in shear strain modulus with the increase of γ. Barros & Hachich (1998) observed that it is common practice to determine G from the curve G/G_{max} *versus* γ, which is obtained using laboratory data, whereas G_{max} is determined through field testing.

3. Carbonate soils

Carbonate soils are the result of the natural sedimentation of particles, comprising biological, mechanical, physical, and chemical processes (Salem et al., 2013). They are characterized by remarkable intraparticle voids (cavities within the soil mass) and irregular shapes of their particles (such as curved plates and hollow tubes), originated from fragments of seashells and skeletal remains of small marine microorganisms. Moura & Freitas (2021) showed that the presence of structures with calcium carbonate, whose degradation can give rise to sands of carbonate origin, is quite recurrent around the world but especially common on the Northeastern coast of Brazil. According to Salem et al. (2013), samples of this type of soil subjected to X-ray diffraction revealed the mineralogical constitution of its particles, highly rich in calcium. As shown in Table 1, carbonate sands from Dabaa (Northern coast of Egypt) have 55.4% of CaO content, due to the environment where these soils are formed.

Table 1. Mineralogical composition of a carbonate sand (Salem et al., 2013).

Mineral	Percentage (%)
SiO_2	0.28
TiO_2	0.02
Al_2O_3	0.12
Fe_2O_3	0.02
MnO	< 0.01
MgO	0.2
CaO	55.4
Na_2O	< 0.01
K_2O	0.02
P_2O_5	0.06
SO_3	0.12
Cl	< 0.01
Ignition loss	43.53

The void ratio (e) of sands normally varies between 0.20 and 0.50 when they are more compact and between 0.8 and 1.2 when loose (Kullhawy & Mayne, 1990). Cataño (2006) carried out 13 tests on carbonate sands, changing their compactness state and determining e. The authors concluded that e for carbonate sands was higher than for typical sands, varying between 0.5 and 1.6 for the most compact states and between 1.1 and 2 for loose condition.

The specific gravity (G_s) is a property of the solid particles of a soil and is strongly linked to its mineralogy. Salem et al. (2013) stated that quartz sands have a G_s of 2.65, whereas carbonate sands usually have higher values, such as calcite (2.75) and aragonite (2.95). Table 2 presents the physical indexes of carbonate sands from different locations cited in the literature.

4. Dynamic parameters for carbonate sands and related research

Jafarian & Javdanian (2019) carried out dynamic and cyclic tests on carbonate sands of the Persian Gulf (Iran), verifying the influence of relative density (D_r) and confining stress ($\sigma\prime_c$) on soil dynamic parameters. Their tests were performed at confining stress of 40, 200, and 400 kPa, and relative densities of 50% and 80%.

In their study, resonant column tests were used to obtain soil dynamic parameters for shear strains between 10^{-4}% and 10^{-2}% and cyclic triaxial tests for shear strains of 10^{-2}% to 1%. The maximum shear modulus was obtained for small strains ($\sim 10^{-4}$%) through the resonant column test.

From there, Jafarian & Javdanian (2019) analyzed in a graph the effects of varying relative density and confining stress on the normalized shear modulus (G/G_{max} curve) and on the damping ratio, for compact state ($D_r = 80$%) and loose state ($D_r = 50$%). They concluded that the dynamic properties G_{max} and D are minimally influenced by the relative density D_r. Also, if the effective confining stress increases, the maximum shear modulus increases and the damping ratio decreases.

In a study on carbonate sands from Nansha (Southern China), Kuang et al. (2020) verified the influence of grain-size distribution on the friction angle through triaxial tests, concluding that for carbonate sands friction angle increases as particle size decreases.

Table 2. Physical indexes of carbonate sands (Salem et al., 2013).

Origin	G_s	D_{10} (mm)	C_u	e_{min}	e_{max}
North Coast (Puerto Rico)	2.79	0.15	2.4	0.75	1.04
Cabo Rojo (Puerto Rico)	2.86	0.2	1.05	1.34	1.71
Playa Santa (Puerto Rico)	2.75	0.16	2.75	0.8	1.22
Dogs Bay (Ireland)	2.75	0.24	2.06	0.98	1.83
Ewa Plains (United States)	2.72	0.2	5.05	0.66	1.3

The literature presents several proposals to predict soil dynamic parameters, for example: Hardin & Drnevich (1972), Ishibashi & Zhang (1993), Ishihara (1996), Rollins et al. (1998), Darendeli (2001), and Oztoprak & Bolton (2013).

The hyperbolic model proposed by Ishihara (1996) has been widely used to describe the nonlinear stress-strain behavior of a wide variety of soils (Kondner & Zelasko, 1963; Duncan & Chang, 1970) and used in the Theory of Plasticity to implement laws for material hardening (Vermeer, 1978). It is a model recognized as the cornerstone for several other studies and models developed on the dynamic response of sands.

Equation 1 shows the hyperbolic model expression for G/G_{max} and Equation 2, for damping ratio, both expressed in terms of the shear strain. In Equation 1 and Equation 2, γ_r is the reference shear strain when $G/G_{max} = 0.5$.

$$\frac{G}{G_{max}} = \frac{1}{1 + \gamma / \gamma_r} \qquad (1)$$

$$D = \frac{4}{\pi} \bullet \left[1 + \frac{1}{\gamma / \gamma_r} \right] \bullet \left[1 - \frac{\ln\left(1 + \gamma / \gamma_r\right)}{\gamma / \gamma_r} \right] - \frac{2}{\pi} \qquad (2)$$

On the other hand, Ishibashi & Zhang (1993) evaluated experimental data regarding the dynamic shear modulus and damping ratio for several types of soils, including sands and clays of high plasticity. The equations developed for G/G_{max} and D are expressed in terms of shear strain, confining effective stress, and plasticity index (PI). In this model, Equations 3-5 can be used to determine G/G_{max}, and Equation 6 to determine the damping ratio of non-cohesive soils (as the carbonate sands).

$$\frac{G}{G_{max}} = k\left(\gamma\right) \bullet \sigma_0'^{\left[m(\gamma) - m_0\right]} \qquad (3)$$

$$k\left(\gamma\right) = 0,5 \bullet \left[1 + \tanh\left\{ \ln\left(\frac{0.00012}{\gamma} \right)^{0.492} \right\} \right] \qquad (4)$$

$$m\left(\gamma\right) - m_0 = 0.272 \bullet \left[1 - \tanh\left\{ \ln\left(\frac{0.000556}{\gamma} \right)^{0.4} \right\} \right] \qquad (5)$$

$$D = 0.333 \bullet \left\{ 0.586 \bullet \left(\frac{G}{G_{máx}} \right)^2 - 1.547 \bullet \left(\frac{G}{G_{máx}} \right) + 1 \right\} \qquad (6)$$

5. Method

In order to develop the equations, the study site was chosen and the characterization of the soil was performed.

In this study, two equations are presented to predict the dynamic behavior of carbonate sands: (1) G/G_{max} *versus* γ; and (2) D *versus* γ. The expressions were obtained using multiple linear regression and data from resonant column tests carried out in a carbonate sand from Cataño & Pando (2010).

5.1 Study site

The soil assessed in this study was a carbonate sand from Cabo Rojo, southwest of Puerto Rico, which was tested by Cataño & Pando (2010). They performed characterization and dynamic tests, including resonant column tests, and obtained the physical properties and the dynamic parameters (maximum shear modulus and damping ratio), as well as the curves G/G_{max} *versus* γ and D *versus* γ.

The studied carbonate sand was poorly graded, with fine to medium grain size, comprising grains between 0.2 mm and 2 mm and without any fines. Table 3 presents its physical properties, with higher G_s and e than the usual values for quartz sands, which implied lower maximum and minimum specific weights.

For more works related to the dynamic behavior of carbonate sands, the following works are cited: Giretti et al. (2018), Liu et al. (2020) and Zhou et al. (2020).

6. Proposals of correlations for shear modulus and damping

6.1 Relations *G versus* γ and *D versus* γ

In order to determine the correlations, the authors used the data presented in Cataño & Pando (2010), which obtained G/G_{max} *versus* γ curves through resonant column tests performed in the carbonate sands of Cabo Rojo.

The correlations were based on two different relative densities: loose (relative compactness between 21% and 26%) and compact (relative compactness of 91%). The tests were carried out considering two effective confining stress levels (50 and 300 kPa).

6.2 Development of proposed equations

The development of the equations G/G_{max} *versus* γ and D *versus* γ sought to establish mathematical relationships between G/G_{max} and D and the shear strain, as a function of

Table 3. Physical properties of the carbonate sand used in this study (Cataño & Pando, 2010).

G_s	e_{max}	e_{min}	% CaCO$_3$
2.86	1.71	1.34	92.8%

explanatory variables. Very few models present expressions as a function of more than one explanatory variable (in addition to γ) and one of them is the hyperbolic model proposed by Ishihara (1996), which considers solely the relative shear strain (γ / γ_r).

In order to develop the equations here proposed, a generic expression (Equation 7) was used to represent the multiple linear regression, i.e., the linear relationship between a dependent variable (y) and two or more independent variables ($x_1, x_2, ..., x_k$). In Equation 7, a_0 is the intercept y (or the value of y) when all the independent variables are zero, while a_1, a_2 and a_k are the coefficients of the independent variables.

$$y = a_0 + a_1 \cdot x_1 + a_2 \cdot x_2 + \ldots + a_k \cdot x_k \tag{7}$$

Since multiple linear regressions involve calculations of complex nature, impractical to be performed manually (Triola, 2008), an electronic spreadsheet was used to process them. The independent variables used in this study were relative density D_r (the compactness state in which the carbonate sand was found), effective confining stress σ'_0 (the stress state to which the material was subjected), and shear strain, which has a great influence on the dynamic response.

Initially, equations correlating G/G_{max} and D with the independent variables were proposed (Equations 8-9).

$$\frac{G}{G_{max}} = a_0 \cdot D_r^{a_1} \cdot \sigma_0'^{a_2} \cdot \left(\frac{1}{1+\gamma}\right)^{a_3} \tag{8}$$

$$D = a_0' \cdot D_r^{a_1'} \cdot \sigma_0'^{a_2'} \cdot \gamma^{a_3'} \tag{9}$$

Using values obtained from the curves G/G_{max} versus γ and D versus γ in Cataño & Pando (2010) for the independent variables, the coefficients $a_0, a_1, a_2, a_3, a'_0, a'_1, a'_2,$ and a'_3 were determined through multiple linear regression. And since the variables $D_r, \sigma'_0,$ and γ are nonlinearly related to G/G_{max} and D, a logarithmic transformation was used to proceed with the multiple linear regression (Equations 10-11).

$$\ln\left(\frac{G}{G_{max}}\right) = \ln a_0 + a_1 \cdot \ln D_r + a_2 \cdot \ln \sigma_0' + a_3 \cdot \ln\left(\frac{1}{1+\gamma}\right) \tag{10}$$

$$\ln(D) = \ln a_0' + a_1' \cdot \ln D_r + a_2' \cdot \ln \sigma_0' + a_3' \cdot \ln \gamma \tag{11}$$

Important to mention that points 1 to 4 in Table 4 (see below) were obtained from Cataño & Pando (2010) and spared to later validate the proposed equations (the validation dataset, *not* used in the development step).

6.3 Proposal for the equation G/G_{max} versus γ and validation

The coefficients of Equation 8 were determined using multiple linear regression in an electronic spreadsheet. Results are shown in Table 5. The obtained expression for G/G_{max} versus γ is shown in Equation 12 and its coefficient of determination (R^2) was 0.87.

$$\frac{G}{G_{max}} = 0.42886 \cdot D_r^{-0.048698} \cdot \sigma_0'^{0.20891} \cdot \left(\frac{1}{1+\gamma}\right)^{13.2937} \tag{12}$$

As previously mentioned, in order to validate Equation 12, some experimental values (points 1 to 4 in Table 4) presented by Cataño & Pando (2010) were considered as a reference and not used in the development of the equations. The comparison between the experimental values and the predicted G/G_{max} (obtained with the proposed equation) is presented in Table 6 and Figure Figure 1.

The results of the proposed expressions (Equation 12) agreed fairly well (error < 10%) with the experimental values presented in Cataño & Pando (2010) for the carbonate sands evaluated in this study, both for soft and compact states.

Figure 2 shows the curves G/G_{max} versus γ obtained by applying the expression proposed in this study to estimate G/G_{max} versus γ (i.e., Equation 12). By analyzing Figure 2, it can be observed that, for $\sigma'_c = 50$ kPa, the equation underestimated G/G_{max} for lower shear strains but had a good convergence for higher values. For $\sigma'_c = 100$ kPa, the same trends were also found.
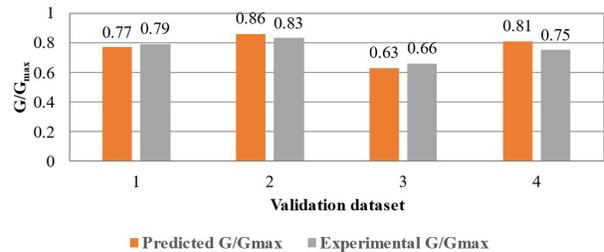
Figure 1. Comparison between predicted and experimental values for G/G_{max}.

Table 4. Test results used in the validation step of the proposed equations [adapted from Cataño & Pando (2010)].

Point	D_r (%)	σ'_c (kPa)	γ (%)	G (MPa)	D (%)
1	21 - 26	50	6×10^{-3}	34.23	3.17
2	21 - 26	300	2.6×10^{-2}	110.2	1.89
3	91	50	1.6×10^{-2}	47.37	3.62
4	91	300	2.6×10^{-2}	119.91	3.16
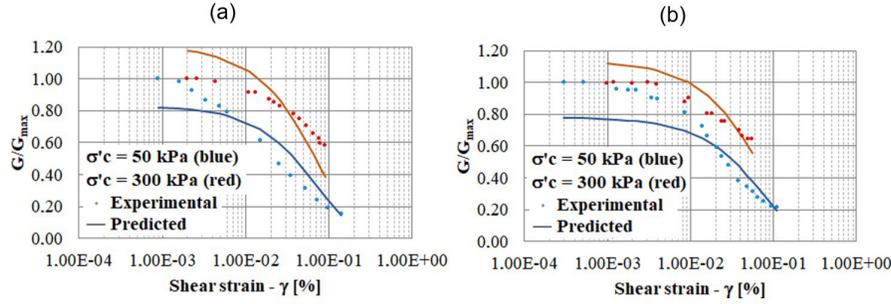
Figure 2. Comparison between the prediction for G/G_{max} and experimental values considering (a) $D_r = 24\%$ and (b) $D_r = 91\%$.

Table 5. Coefficients obtained for equation G/G_{max} versus γ.

a_0	a_1	a_2	a_3
0.42886	-0.048698	0.20891	13.2937

Table 6. Validation of the proposed equation G/G_{max} versus γ.

Point	Predicted G/G_{max}	Experimental G/G_{max}	$\Delta[\%]$
1	0.77	0.79	-2.53
2	0.86	0.83	+3.61
3	0.63	0.66	-4.55
4	0.81	0.75	+8

Table 7. Coefficients obtained for equation D versus γ.

a_0	a_1	a_2	a_3
103.61	0.076315	-0.40996	0.50658

Table 8. Validation of the proposed equation D versus γ.

Point	Predicted D	Experimental D	$\Delta[\%]$
1	1.99	3.17	-37.22
2	2.01	1.89	+6.35
3	3.62	3.62	0
4	2.22	3.16	-29.75

6.4 Proposal for the equation *D versus γ* and validation

Similarly, the coefficients of Equation 9 were determined using multiple linear regression in an electronic spreadsheet. Results are shown in Table 7. The obtained expression for *D versus γ* is shown in Equation 13 and its R^2 was 0.92.

$$D = 103.61 \cdot D_r^{0.076315} \cdot \sigma_0'^{-0.40996} \cdot \gamma^{0.50658} \qquad (13)$$

Similarly, when validating Equation 13, some experimental values (points 1 to 4 in Table 4) from Cataño & Pando (2010) were also taken as a reference and not
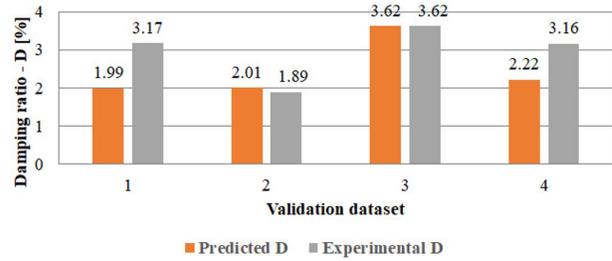
Figure 3. Comparison between predicted and experimental values for *D*.

used in the development step. The comparison between the predicted and the experimental values for *D* is shown in Table 8 and Figure 3.

Based on Table 8 and Figure 3, one can observe that there were differences between predicted and experimental values of *D* of up to 37.22%. On the other hand, two of the four predictions presented very small to negligible differences.

Figure 4 shows the new curves *D versus γ* obtained by applying the expression proposed in this study to estimate *D versus γ* (i.e., Equation 13). Based on the graphs, the proposed equation provided satisfactory concordant predictions when compared with experimental values. However, the expression showed a trend to underestimate predictions for loose sands ($D_r = 24\%$) and effective confining stress of 50 kPa.

6.5 Comparison between predictions of the proposed equations and experimental values from Javdanian & Jafarian (2018)

Javdanian & Jafarian (2018) tested a carbonate sand from the Island of Hormuz, a seismic region of the Persian Gulf, in Iran. They studied the dynamic behavior of that sand through resonant column and cyclic triaxial tests, considering effective confining stress of 200, 400, and 800 kPa, and obtaining the curves G/G_{max} *versus γ* and *D versus γ*. The physical indexes of the referred carbonate sand are $G_s = 2.73$, $\gamma_{max} = 18.1$ kN/m³ and $\gamma_{min} = 16.1$ kN/m³.

Predictions of the proposed equations on the dynamic parameters for the carbonate sand from the Island of Hormuz were evaluated and then compared with the experimental
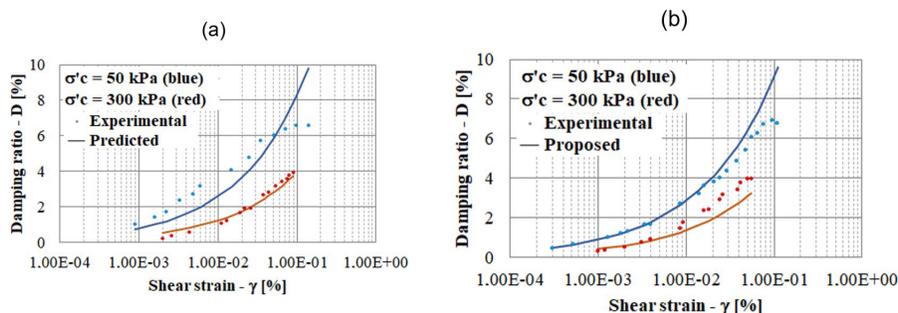
(a)

(b)

Figure 4. Comparison between the prediction for *D* and experimental values considering D_r = 24% (a) and D_r = 91% (b).
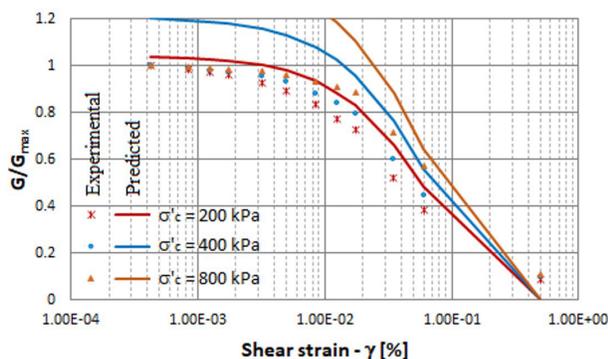

Figure 5. Comparison between predictions for G/G_{max} using proposed equations and experimental data for the carbonate sand from Javdanian & Jafarian (2018).
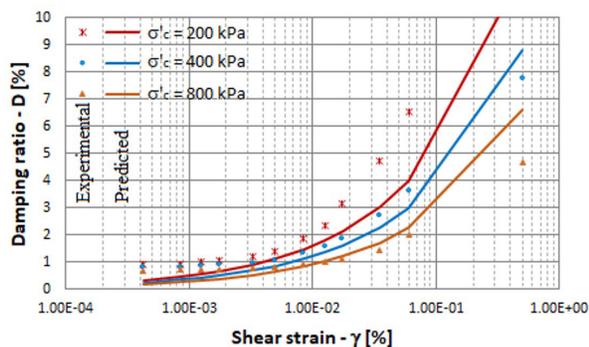

Figure 6. Comparison between predictions and experimental values for *D versus* γ of the carbonate sand from Javdanian & Jafarian (2018).

data presented in the study by Javdanian & Jafarian (2018). Figures 5-6 show the predicted and experimental curves for G/G_{max} *versus* γ and *D versus* γ of the aforementioned carbonate sand, in which solid lines represent the predictions obtained with the proposed expressions and the markers correspond to laboratory data.

From Figure 5, it can be observed that, in general, predicted values for G/G_{max} were a little overestimated when compared with experimental data (Δ of up to 32%), especially

for smaller shear strains (12%). This can be explained by the fact that the expression here presented (Equation 6) was developed based on experimental data obtained from tests carried out at low confining stress (50 to 300 kPa). Thus, for scenarios of higher confining stress, as in this case, less convergent results can be accepted.

Figure 6 shows that the predicted values for the damping ratio were in fair agreement with the experimental data from Javdanian & Jafarian (2018), even for effective confining stress higher than the range used to develop Equation 9, proposed in this study.

7. Conclusions

The carbonate sand from Cabo Rojo (Puerto Rico) evaluated in Cataño & Pando (2010) presented different physical indexes when compared to common quartz sands. Both G_s and void ratio were higher than typical values for quartz sands, which implied lower maximum and minimum specific weights.

In this study, multiple linear regression was used to determine equations to predict the curves G/G_{max} *versus* γ and *D versus* γ for carbonate sands, reaching coefficients of determination (R^2) of 0.87 and 0.92, respectively.

The predictions regarding the relationship G/G_{max} *versus* γ showed good agreement with the experimental values obtained by Cataño & Pando (2010), with an average error of less than 10% (in relation to reference/experimental values). For *D versus* γ, the proposed equation also presented concordant results, with a slight trend to underestimation but mainly for the loose condition (D_r = 24%) of the sands and lower effective confining stress (50 kPa).

Predictions on the dynamic parameters using the equations proposed in this study were also compared with the experimental results of a carbonate sand from Iran (Javdanian & Jafarian, 2018). The predictions for the damping ratio agreed with the experimental data regardless of the effective confining stress, a fact not observed for the curve G/G_{max} *versus* γ, which presented good results only for the confining stress of 200 kPa. The highest variation obtained for G/G_{max} was 32% for higher confining stresses and less than 12% for lower confining stresses.

Acknowledgements

Declaration of interest

The authors have no conflicts of interest to declare. All co-authors have observed and affirmed the contents of the paper and there is no financial interest to report.

Authors' contributions

Felipe Oscar Pinto Barroso: conceptualization, funding acquisition, investigation, data curation, methodology, software, visualization, writing – original draft. Alfran Sampaio Moura: conceptualization, formal analysis, funding acquisition, data curation, supervision, validation, writing – review & editing.

Data availability

Data analyzed in the course of the current study are available in the GeoFlorida 2010 repository, https://doi.org/10.1061/41095(365)83.

List of symbols

a_0, a_1, a_2, a_3:	coefficients of the multiple linear regression
e:	void ratio
e_{max}:	maximum void ratio
e_{min}:	minimum void ratio
v_R:	Rayleigh wave velocity
v_s:	shear wave velocity
C_u:	coefficient of uniformity
D:	damping ratio
D_r:	relative density
D_{10}:	soil effective diameter
G:	shear modulus
G_{max}:	maximum shear modulus
G_s:	specific gravity
R^2:	coefficient of determination
SPT:	standard penetration test
γ:	shear strain
γ_r:	reference shear strain when $G/G_{max} = 0.5$
γ_{max}:	maximum specific weight
γ_{min}:	minimum specific weight
σ'_c or σ'_0:	confining effective stress
Δ:	percentage variation

References

Barros, J.M.C., & Hachich, W. (1998). Fundações sujeitas a esforços dinâmicos. In W.C. Hachich & F.F. Falconi (Eds.), *Fundações: teoria e prática* (pp. 409-442). Pini.

Cataño, A.J. (2006). *Stress strain behavior and dynamic properties of Cabo Rojo calcareous sands* [Master's dissertation, University of Puerto Rico]. University of Puerto Rico's repository. Retrieved in December 22, 2022, from https://scholar.uprm.edu/handle/20.500.11801/1782?show=full

Cataño, A.J., & Pando, M.A. (2010). Static and dynamic properties of a calcareous sand from Southwest Puerto Rico. In D.O. Fratta, A.J. Puppala & B. Muhunthan (Eds.), *GeoFlorida 2010: Advances in Analysis, Modeling & Design* (pp. 842-851). Reston, United States of America: American Society of Civil Engineers. https://doi.org/10.1061/41095(365)83.

Darendeli, B.M. (2001). *Development of a new family of normalized modulus reduction and material damping curves* [Doctoral thesis, The University of Texas at Austin]. The University of Texas at Austin's repository. Retrieved in December 22, 2022, from http://hdl.handle.net/2152/10396

Duncan, J.M., & Chang, C.Y. (1970). Nonlinear analysis of stress and strain in soils. *Journal of the Soil Mechanics and Foundations Division*, *96*(5), 1629-1653. http://dx.doi.org/10.1061/JSFEAQ.0001458.

Giretti, D., Fioravante, V., Been, K., & Dickenson, S. (2018). Mechanical properties of a carbonate sand from a dredged hydraulic fill. *Geotechnique*, *68*(5), 410-420. http://dx.doi.org/10.1680/jgeot.16.P.304.

Hardin, B.O., & Drnevich, V.P. (1972). Shear modulus and damping in soils: design equations and curves. *Journal of the Soil Mechanics and Foundations Division*, *98*(7), 667-692. http://dx.doi.org/10.1061/JSFEAQ.0001760.

Hyodo, M., Aramaki, N., Itoh, M., & Hyde, A.F.L. (1996). Cyclic strength and deformation of crushable carbonate sand. *Soil Dynamics and Earthquake Engineering*, *15*(5), 331-336. http://dx.doi.org/10.1016/0267-7261(96)00003-6.

Ishibashi, I., & Zhang, X. (1993). Unified dynamic shear moduli and damping ratios of sand and clay. *Soil and Foundation*, *33*(1), 182-191. http://dx.doi.org/10.3208/sandf1972.33.182.

Ishihara, K. (1996). *Soil behaviour in earthquake geotechnics*. Oxford University Press.

Jafarian, Y., & Javdanian, H. (2019). Dynamic properties of calcareous sand from the Persian Gulf in comparison with siliceous sands database. *International Journal of Civil Engineering*, *18*, 245-249. http://dx.doi.org/10.1007/s40999-019-00402-9.

Javdanian, H., & Jafarian, Y. (2018). Dynamic shear stiffness and damping ratio of marine calcareous and siliceous sands. *Geo-Marine Letters*, *38*, 315-322. http://dx.doi.org/10.1007/s00367-018-0535-9.

Kondner, R.L., & Zelasko, J.S. (1963). A hyperbolic stress-strain formulation of sands. In Associação Brasileira de Mecânica dos Solos (Ed.), *Proceedings of the Second Panamerican Conference on Soil Mechanics and Foundation Engineering* (pp. 289-324). São Paulo, Brazil: Associação Brasileira de Mecânica dos Solos.

Kuang, D., Long, Z., Wang, J., Zhou, X., & Yu, P. (2020). Experimental study on particle size effect on mechanical behaviour of dense calcareous sand. *Soils and Rocks*, *43*(9), 567-574. http://dx.doi.org/10.28927/SR.434567.

Kullhawy, F.H., & Mayne, P.H. (1990). *Manual on estimating soil properties for foundation design*. Cornell University.

Liu, X., Li, S., & Sun, L. (2020). The study of dynamic properties of carbonate sand through a laboratory database. *Bulletin of Engineering Geology and the Environment*, *79*, 3843-3855. http://dx.doi.org/10.1007/s10064-020-01785-z.

Moura, R.L., & Freitas, M.O. (2021). *Rodolitos: os desconhecidos recifes "rolling stones"*. Retrieved in January 12, 2023, from https://oeco.org.br/analises/rodolitos-os-desconhecidos-recifes-rolling-stones/

Oztoprak, S., & Bolton, M.D. (2013). Stiffness of sands through a laboratory test database. *Geotechnique*, *63*(1), 54-70. http://dx.doi.org/10.1680/geot.10.P.078.

Ponte, G.F., & Moura, A.S. (2017). Avaliação do comportamento dinâmico das fundações superficiais de aerogeradores a partir de ensaios de pequena e grande deformações. *Revista Eletrônica de Engenharia Civil*, *13*(1), 95-105. http://dx.doi.org/10.5216/reec.v13i1.40950.

Rollins, K.M., Evans, M.D., Diehl, N.B., & Daily III, W.D. (1998). Shear modulus and damping relationships for gravels. *Journal of Geotechnical and Geoenvironmental Engineering*, *124*(5), 398-405. http://dx.doi.org/10.1061/(ASCE)1090-0241(1998)124:5(396).

Salem, M., Elmamlouk, H., & Agaiby, S. (2013). Static and cyclic behavior of North Coast calcareous sand in Egypt. *Soil Dynamics and Earthquake Engineering*, *55*, 83-91. http://dx.doi.org/10.1016/j.soildyn.2013.09.001.

Sharma, S.S., & Ismail, M.A. (2006). Monotonic and cyclic behavior of two calcareous soils of different origins. *Journal of Geotechnical and Geoenvironmental Engineering*, *132*(12), 1581-1591. http://dx.doi.org/10.1061/(ASCE)1090-0241(2006)132:12(1581).

Triola, M.F. (2008). *Introdução à estatística*. LTC.

Vermeer, P.A. (1978). A double hardening model for sand. *Geotechnique*, *28*(4), 413-433. http://dx.doi.org/10.1680/geot.1978.28.4.413.

Zhou, X.Z., Chen, Y.M., Liu, H.L., & Zhang, X.L. (2020). Experimental study on the cyclic behavior of loose calcareous sand under linear stress paths. *Marine Georesources and Geotechnology*, *38*(3), 277-290. http://dx.doi.org/10.1080/1064119X.2019.1567631.